BRILL

CONTRIBUTIONS TO ZOOLOGY (2025) 1–18

CTOZ

brill.com/ctoz

Morphological Divergence in Marbled and Pygmy Newts: A Skull Shape Perspective

Ana Ivanović | ORCID: 0000-0002-6247-8849
University of Belgrade, Faculty of Biology
ana@bio.bg.ac.rs

Tijana Vučić | ORCID: 0000-0002-8850-5251
Biology, Leiden University, Sylviusweg 72, 9 2333 BE Leiden, The Netherlands
Corresponding author
t.vucic@biology.leidenuniv.nl

Jan W. Arntzen | ORCID: 0000-0003-3229-5993
Institute of Biology, Leiden University, Leiden, The Netherlands
Naturalis Biodiversity Center, Leiden, The Netherlands
pim.arntzen@gmail.com

RECEIVED 11 JULY 2025; ACCEPTED 10 OCTOBER 2025;
PUBLISHED ONLINE 20 NOVEMBER 2025; PUBLISHED IN ISSUE
EDITOR: ALEXANDRA A.E. VAN DER GEER

Abstract

The vertebrate skull integrates vital functions such as feeding, brain protection and sensory perception, making it a key structure for studying morphological evolution. Using micro-computed tomography and geometric morphometrics, we examined skull shape variation in the salamander genus *Triturus*, focusing on five (sub)species within the recently revised *T. marmoratus* species group (marbled and pygmy newts). Results were compared with the sister *T. cristatus* species group (crested newts) which comprises eight species, including a recent diversification within *T. carnifex* documented by molecular data. The two groups, which diverged approximately 28 million years ago, take opposite positions over a shape gradient, from broad skulls with posteriorly positioned jaws to narrower, elongated skulls with more anteriorly positioned jaw articulations, respectively. Both groups exhibit comparable levels of morphological variation (disparity) in skull shape. In the *T. cristatus* species group, skull shape changes are paralleled by changes in axial morphology (with a vertebral count ranging from 13 to 17) whereas species of the *T. marmoratus* group have a uniform count of 12 trunk vertebrae. The subspecies *Triturus m. marmoratus* stands

Published with license by Koninklijke Brill BV | DOI:10.1163/18759866-BJA10084
 | ISSN: 1875-9866 (online)

out from other taxa in its group in jaw articulation and pterygoid placement, and vomerine tooth row lengths – features that suggest functional differences in feeding mechanics or diet. Further research on the function morphology of feeding, feeding regimes and phenology of taxa may help to uncover drivers of morphological divergence.

Keywords

Feeding and food processing – geometric morphometrics – micro-computed tomography – skull morphology – *Triturus cristatus* species group – *Triturus marmoratus* species group

Introduction

The shape of the vertebrate skull is strongly influenced by genetic and developmental factors, constrained by functional demands and is highly adaptive, making it a promising structure for the study of morphological evolution (Cheverud, 1995; Hallgrímsson et al., 2007). Moreover, modern micro-computed tomography in combination with geometric morphometrics enables the precise description of skull shape which assists in elucidating the mechanisms and processes that drive morphological evolution (Sherratt et al., 2014; Bordua et al., 2019; Urosević et al., 2019; Paluh et al., 2020; Kyomen et al., 2023; Sherratt & Kraatz, 2023).

Changes in skull shape of salamandrid salamanders are relatively well studied at both the macroevolutionary (Ivanović & Arntzen, 2018; Fabre et al., 2020) and microevolutionary level (Ivanović & Kalezić, 2012; Üzüm et al., 2015). Special attention went to the large-bodied newt genus *Triturus* (Ivanović et al., 2008, 2013; Cvijanović et al., 2014; Ivanović & Arntzen, 2014), where the majority of evolutionary changes in the skull is concentrated in the otico-occipital region and adjacent bones, along with changes in the relative position of the jaws (Ivanović & Arntzen, 2014). The ten or eleven species in the genus represent five morphotypes in a gradient from stout to slender to which the length of the annual aquatic breeding phase runs in parallel from 2–6 months (Arntzen, 2003; Wielstra et al., 2019). Variation in skull size and shape also shows a clear association with an ecological gradient across *Triturus* species. These patterns suggest that morphological evolution has been shaped in part by series of shifts in the ecological niche (Ivanović & Arntzen, 2014). It has been estimated that the *T. marmoratus* and *T. cristatus* species groups separated from one another 28.4 million years (Mya) ago with a 29.0–22.6 confidence interval (Steward & Wiens, 2025). Recent changes in the taxonomy of the *T. marmoratus* species group (Arntzen, 2024abc, in line with Kazilas et al., 2024) necessitate a revision and extension of the morphometric data published earlier (Ivanović & Arntzen, 2014, 2018). The approximate ranges of *Triturus* species and subspecies are shown in Figure 1, while their phylogenetic relationships and a proposed vernacular nomenclature are presented in Figure 2.

We investigated shape differentiation across the genus *Triturus* and quantified

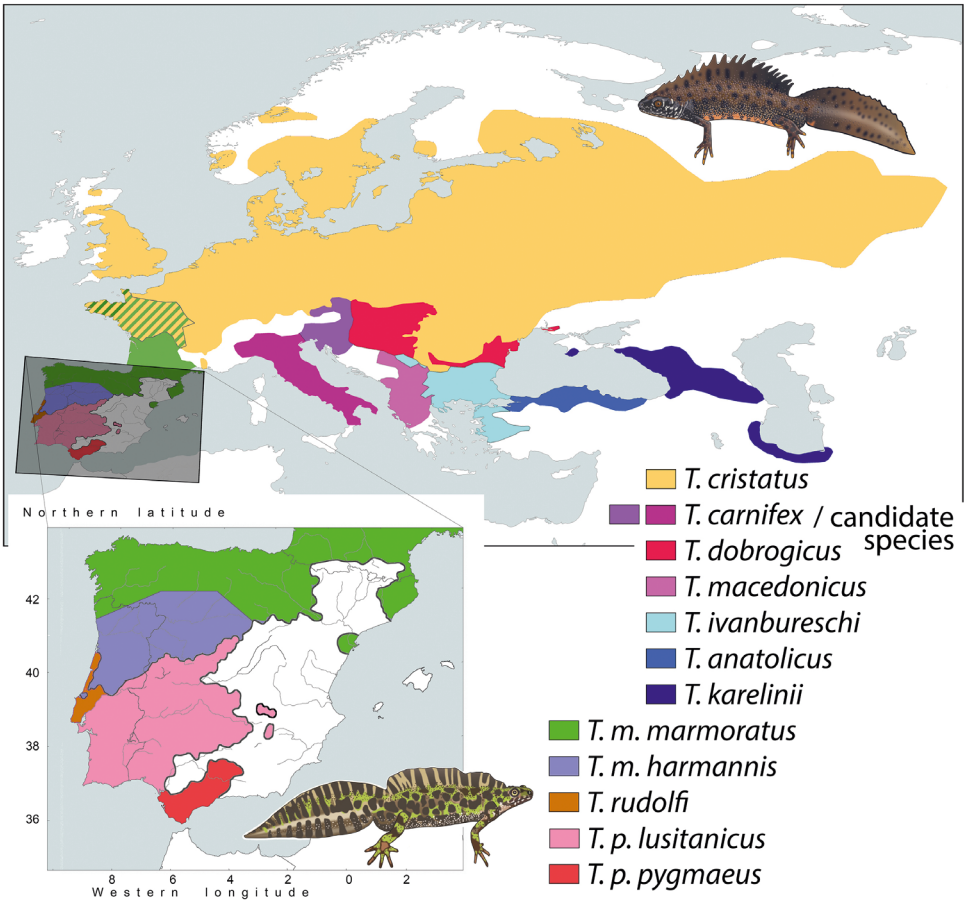

FIGURE 1 Distribution of the genus *Triturus* across Eurasia. Top panel – species in the *T. cristatus* species group. The information on the proposed separation of *T. carnifex* in a Balkan species and an Apennine species yet to be described goes back to Wielstra et al. (2021). Bottom panel – species and subspecies in the *T. marmoratus* species group after (Arntzen, 2024cd). Note that the position and width of the *T. m. marmoratus* – *T. m. harmannis* contact zone and that within *T. carnifex sensu lato* are not yet well established. The animal drawings are by Bas Blankevoort at Naturalis Biodiversity Center.

morphological disparity, defined as among-taxon variance in skull size and shape. Specifically, we aimed to characterize skull shape variation in marbled and pygmy newts (the *T. marmoratus* species group) and to identify potential factors driving the evolution of skull morphology in *Triturus*.

Material and methods

We analyzed micro-CT scan data for 90 newts of the *T. marmoratus* species group (40 marbled newts representing *T. marmoratus marmoratus, T. m. harmannis* and 50 pygmy newts representing *T. pygmaeus pygmaeus*, *T. p. lusitanicus*

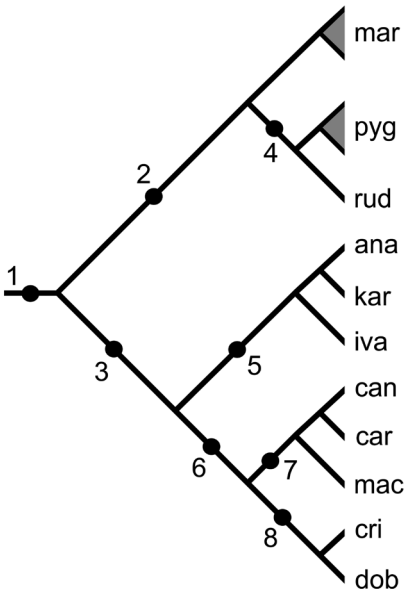

FIGURE 2 Phylogenetic tree of species in the genus *Triturus* (after Wielstra et al., 2013, 2019) along with a proposed vernacular nomenclature. Numbers on the tree refer to: 1 – genus *Triturus* Rafinesque, 1815 – Large bodied newts, 2 – *Triturus marmoratus* species group, 3 – *Triturus cristatus* species group, 4 – Pygmy newts, 5 – Eurasian crested newts, 6 – European crested newts, 7 – Southern European crested newts, including a species yet to be described (cf. Wielstra et al., 2021) and 8 – Elongated crested newts. At the species level names and authorities coming with the three letter codes are as below with proposed vernacular names in square brackets: **ana** – *Triturus anatolicus* Wielstra et Arntzen, 2016 [Anatolian crested newt], **can** – candidate species, sister to *T. carnifex* [Italian crested newt], **car** – *Triturus carnifex* (Laurenti, 1768) [Slovenian crested newt], **cri** – *Triturus cristatus* (Laurenti, 1768) [Northern, or Great crested newt], **dob** – *Triturus dobrogicus* (Kiritzescu, 1903) [Danube crested newt], **iva** – *Triturus ivanbureshi* Arntzen et Wielstra, 2013 [Balkan crested newt], **kar** – *Triturus karelinii* (Strauch, 1870) [Caucasian crested newt], **mac** – *Triturus macedonicus* (Karaman, 1922) [Macedonian crested newt], **mar** – *Triturus marmoratus* (Latreille, 1800) [Marbled newt] with the subspecies *T. m. marmoratus* [Northern marbled newt] and *T. m. harmannis* Arntzen 2024 [Southern, or Harmannis' marbled newt], **pyg** – *Triturus pygmaeus* (Wolterstorff, 1905) [Pygmy newt] with the subspecies *T. p. pygmaeus* [Southern pygmy newt] and *T. p. lusitanicus* Arntzen, 2024 [Northern, or Lusitanian pygmy newt], **rud** – *Triturus rudolfi* Arntzen, 2024 [Malkmus', or Lisbon pygmy newt]. We abandon the designation 'superspecies' (Rensch, 1929; Mayr, 1931, 1943) as applied by Wallis & Arntzen (1981) because the full species status of the members of the *T. cristatus* species group is by now well established (Arntzen et al., 2014). We note that the type locality of *T. carnifex* is Vienna, Austria (Mertens & Müller, 1928) so that the vernacular name 'Italian crested newt' now applies to the candidate species. We furthermore note that with 'Marbled newts' it is meant *T. marmoratus* and subspecies exclusively, i.e., excluding the Pygmy newts *T. pygmaeus* and *T. rudolfi*.

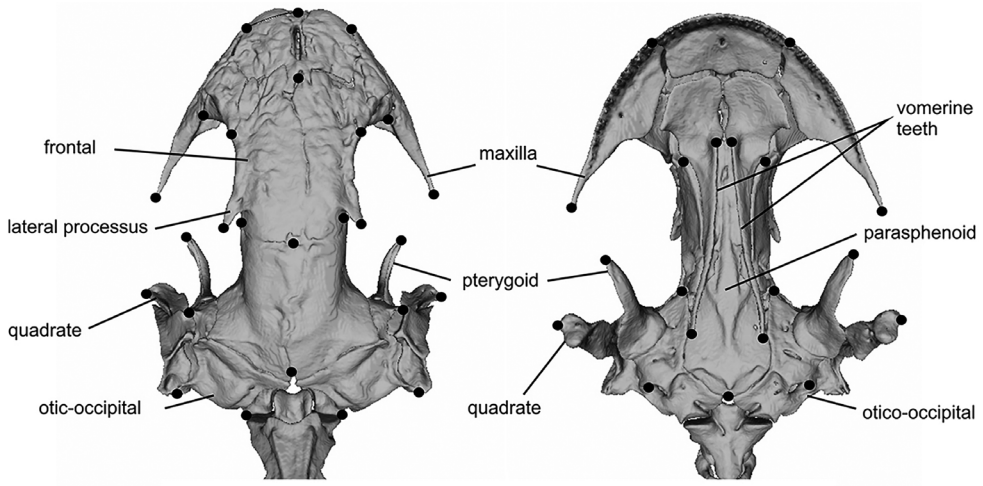

FIGURE 3 Dorsal (left) and ventral (right) view on the surface model of the skull of *Triturus rudolfi* (specimen RMNH.RenA 51786 from Cercal, Portugal). The black dots are landmarks used to characterize skull shape, following Ivanović & Arntzen (2018).

and *T. rudolfi*) and 188 newts of the *T. cristatus* species group (*T. anatolicus, T. carnifex* (including a candidate species), *T. cristatus*, *T. dobrogicus, T. ivanbureschi*, *T. karelinii* and *T. macedonicus*) with taxon sample sizes that ranged from 10 to 35 (Appendix 1). The data were obtained with either a SkyScan 1172 micro-CT scanner (N=264) (Skyscan; Aartselaar, Belgium) or a Neoscan N80 Desktop (N=14) (Merkel Technologies Ltd., Belgium) at Naturalis Biodiversity Center, Leiden, The Netherlands. Representative 3D surface models for each (sub)species of *T. marmoratus* species group are available as supplementary material. We set 39 morphometric landmarks of which five were medians and 17 were bilaterally symmetric (Ivanović & Arntzen, 2018; Fig. 3). The landmark coordinates were obtained directly from the surface models with Landmark IDAV 3.6 software (Landmark, 2005).

Analyses were done using R version 4.4.1 (R Core Team, 2024) with the packages geomorph v. 4.0.10 (Baken et al., 2021; Adams et al., 2025), RRPP v. 2.1.2 (Collyer & Adams, 2018, 2024), dplyr v. 1.1.4 (Wickham et al., 2023) and ggplot v. 3.5.1 (Wickham, 2016). For the entire dataset of landmark configurations, a general Procrustes analysis was performed by using the bilat.symmetry() function, from which the centroid size (CS) was calculated as size variable and the symmetric component was calculated as a shape variable (Dryden & Mardia, 1998; Klingenberg et al., 2002; Rohlf & Slice, 1990). Principal component analyses were done to explore skull shape variation within and between (sub)species of the *T. marmoratus* species group and for the entire genus *Triturus* separately, using the gm.prcomp() function.

We estimated morphological disparity in skull size and shape within the *T. marmoratus* and *T. cristatus* species groups as the Procrustes variance of each species group, using the summarise() function for size and the morphol.disparity()

function for shape. To test for statistically significant differences in disparity between species groups, we applied an *F*-test for size using the var.test() function and a randomised residual permutation procedure (1,000 permutations) for shape using morphol.disparity().

Differences in mean skull size and shape among (sub)species of the *T. marmoratus* species group were evaluated using two permutation-based ANOVAs (for size and shape separately) by using the procD.lm() function, with CS as size variable, the symmetric component as the shape variable and taxon as a factor. To assess statistical significance, we applied the residual randomisation test as above. We used the pairwise() function to assess if there is significant difference between pairs of (sub) species in skull size and shape. To test for the potential effect of size (allometry) on skull shape divergence and to assess significance, we performed a permutation-based MANCOVA with residual randomisation, again under 1,000 permutations. The symmetric component was used as the shape variable, (sub)species as the factor, CS as the covariate, and the taxon × CS interaction to evaluate differences in allometric slopes using the procD.lm() function.

Results

An exploratory principal componet (PC) analysis performed on the entire genus *Triturus* showed that most variation in skull shape, expressed along the first PC axis (that accounts for approximately 28% of the total variance in the data) is related to variation in the relative length and width of the skull, particularly in the otico-occipital region. Skull shape varies from short and wide with wider and posteriorly positioned quadrates (i.e., the jaw articulation) in *T. m. harmannis* to narrow and elongated with narrower and more anteriorly positioned jaws in *T. dobrogicus* (Fig. 4). The lateral processes of the frontal bones are more pronounced and positioned more posteriorly in the *T. marmoratus* than in the *T. cristatus* species group. The second PC axis (describing approximately 9% of total variance) describes the variation in relative length of the vomerine tooth rows, from elongated and parallel that almost reach the posterior end of parasphenoids to shorter vomerine tooth rows in *T. marmoratus* and *T. dobrogicus* where they reach from half to two-third of the parasphenoid length.

The *T. marmoratus* and *T. cristatus* species groups differ significantly in skull size disparity, with greater variation in crested newts (size disparity = 15.80) than in marbled newts (size disparity = 9.12). This difference is statistically supported by an *F*-test ($F = 1.739$, $df_1/_2 = 187/89$, $P < 0.01$). However, there is no statistically significant difference in the morphological disparity of skull shape between *T. marmoratus* and *T. cristatus* species groups (shape disparity is 0.0060 in crested newts and 0.0062 in marbled newts; $P > 0.05$).

A separate PC analysis conducted on the *T. marmoratus* species group revealed that the first, second and third principal components (together accounting for approximately 39% of the total shape variance) describe most of the differences among the five taxa (Fig. 5). The first axis (explaining approximately 19% of the variance) resolves *T. m. marmoratus*

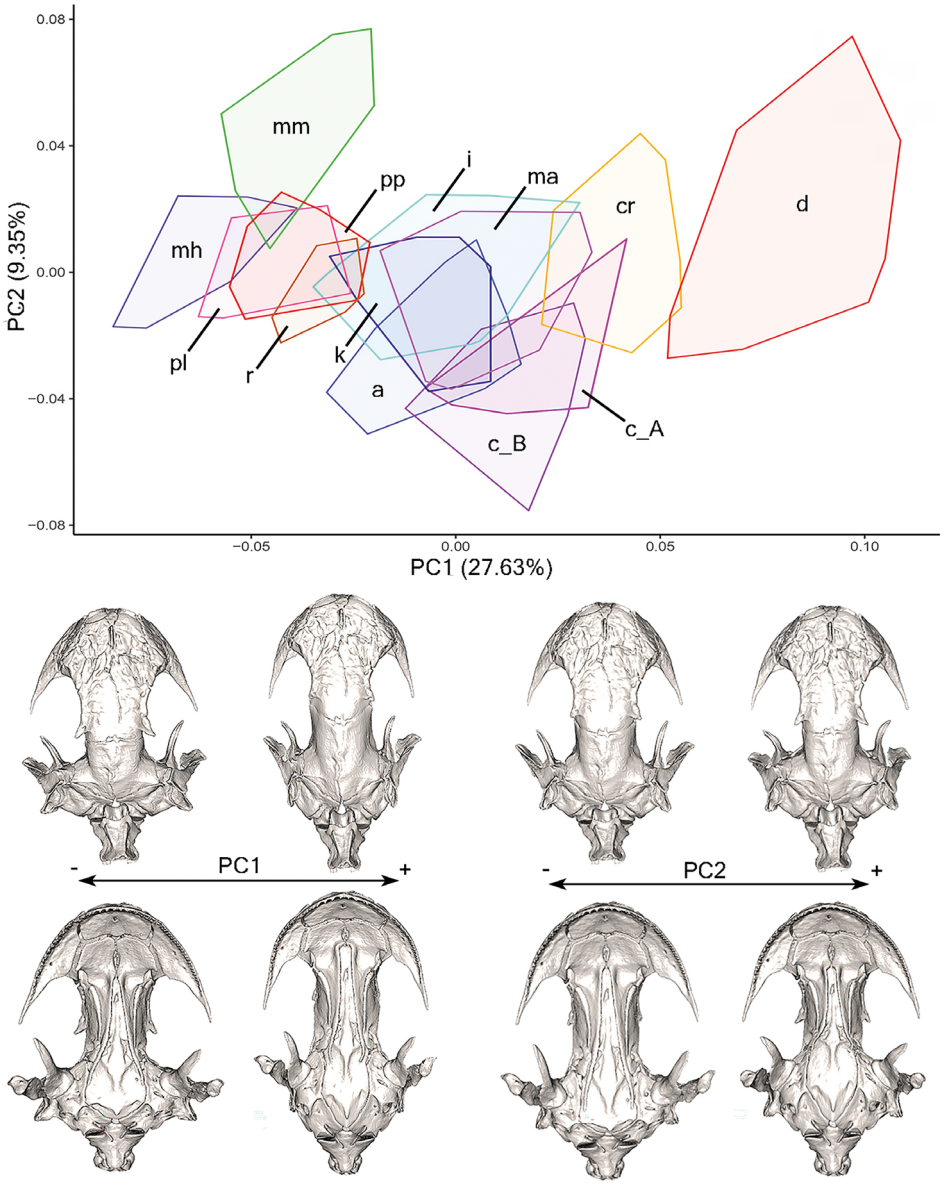

FIGURE 4 Skull morphology in *Triturus* newts. Top panel – principal component (PC) analysis of the symmetric component of skull shape in 278 individuals, color-coded by (sub)species as in Figure 1, with convex outside polygons summarizing the space taken over the first and second PC-axis. Species and subspecies are labeled as: a – *T. anatolicus*, c_A – candidate species from the Apennine Peninsula , c_B – *T. carnifex* from Slovenia and adjacent areas, cr – *T. cristatus*, d – *T. dobrogicus*, i – *T. ivanbureschi*, k – *T. karelinii*, ma – *T. macedonicus*, mh – *T. m. harmannis*, mm – *T. m. marmoratus*, pl – *T. p. lusitanicus*, pp – *T. p. pygmaeus* and r – *T. rudolfi*. Bottom panel – Three-dimensional surface models illustrating shape changes along first and second principal axis. Dorsal views are presented above, and ventral views below the corresponding two-headed arrows.

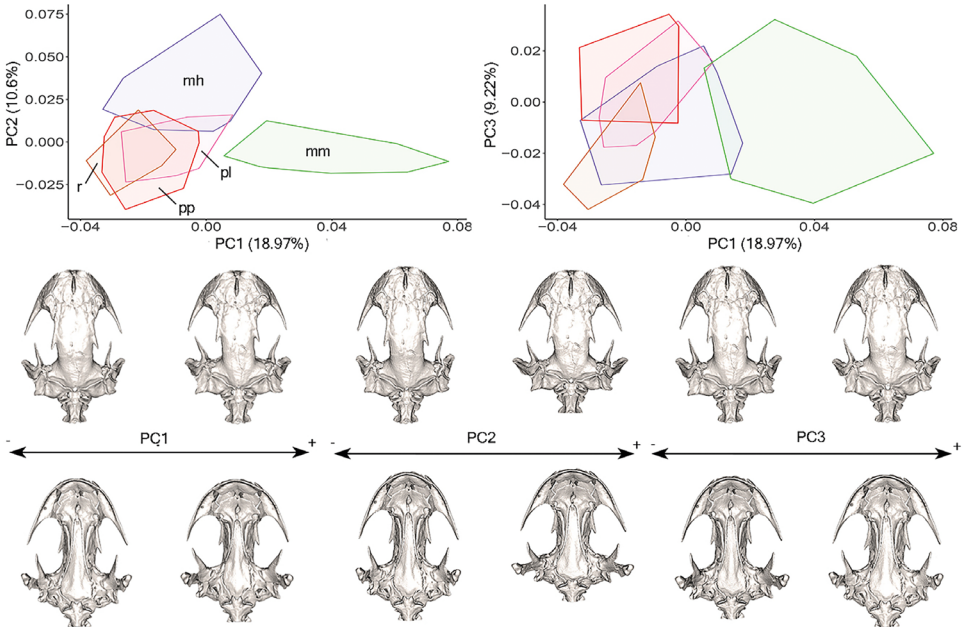

FIGURE 5 Skull morphology in marbled and pygmy newts. Top panel – Principal component analysis of the symmetric component of skull shape in 90 marbled and pygmy newts. Polygons represent the distribution of (sub)species in shape space and are color coded as in Figure 1 with labels: mh – *T. m. harmannis*, mm – *T. m. marmoratus*, r – *T. rudolfi*, pl – *T. p. lusitanicus* and pp – *T. p. pygmaeus*. Bottom panel – three-dimensional surface models illustrating shape changes along the first three principal component axes shown in the top panel. Dorsal views are presented above, and ventral views below, the corresponding two-headed arrows.

as different from the others; the second axis (accounting for approximately 11%) resolves *T. m. harmannis* as different from the remainder whereas *T. p. pygmaeus*, *T. p. lusitanicus* and *T. rudolfi* remain undifferentiated. *Triturus m. marmoratus* stands out by shorter vomerine tooth rows, a wider skull and a more laterally positioned pterygoid. *Triturus m. harmannis* stands out by a shorter otic-occipital region and a skull that is wider at the jaw articulation point. *Triturus p. pygmaeus*, *T. p. lusitanicus* and *T. rudolfi* gradually differentiate along the third axis (variance approximately 9%). Individuals of *T. rudolfi* possess a narrower and more elongated skull, with shorter maxillary bones and a more posteriorly positioned squamosal–otic-occipital suture compared to *T. pygmaeus*. Statistically significant differences in skull shape among taxa were detected by permutational ANOVA (df = 4, SS = 0.082, R^2 = 0.268, F = 7.786, Z = 9.46, P < 0.001). Post hoc pairwise comparisons revealed differences in skull shape between taxa to be statistically highly significant (P < 0.001), but less so for *T. p. lusitanicus* versus *T. p. pygmaeus* (P < 0.05) and *T. p. pygmaeus* versus *T. rudolfi* (P < 0.01).

Size comparisons showed significant differences in skull size among (sub)species of the *T. marmoratus* species group

(ANOVA: df = 4, SS = 408.64, F = 21.57, P < 0.001). Pairwise comparisons revealed that both *T. marmoratus* subspecies have significantly larger skulls than both *T. pygmaeus* subspecies and *T. rudolfi*. However, no significant differences in skull size were found within *T. marmoratus* (mean values of CS ± standard deviation: *T. m. marmoratus*, 32.64 ± 2.02 and *T. m. harmannis*, 32.83 ± 3.12, P > 0.05) or within *T. pygmaeus* (*T. p. pygmaeus*, 27.67 ± 1.98 and *T. p. lusitanicus*, 28.75 ± 1.64, P > 0.05). *Triturus rudolfi* (30.04 ± 2.40) has a significantly larger skull than *T. p. pygmaeus* (P < 0.05) but does not differ significantly from *T. p. lusitanicus* (P > 0.05). The MANCOVA analysis showed a significant taxon × CS interaction, indicating that the (sub)species significantly diverge in size-related shape changes (df = 4, SS = 0.0150, R^2 = 0.05, F = 1.50, Z = 3.01, P < 0.01).

Discussion

Morphological diversification in the genus *Triturus* is well established and follows an ecological/behavioural gradient, ranging from predominantly terrestrial to increasingly aquatic modes of life (Arntzen, 2003; Ivanović & Arntzen, 2014; Wielstra et al., 2019). Species differ markedly in body proportions (Wolterstorff, 1923) and in the number of trunk vertebrae, forming five distinct vertebral morphotypes (Arntzen et al., 2015). All (sub) species of the *T. marmoratus* group share a single morphotype with 12 trunk vertebrae. In contrast, the *T. cristatus* species group exhibits substantial variation: the stout, long-legged *T. karelinii* and its allies *T. ivanbureschi* and *T. anatolicus* have 13 vertebrae, *T. macedonicus* and *T. carnifex* (*sensu lato*) have 14, *T. cristatus* has 15, and the elongated, short-legged *T. dobrogicus* has 16 or 17 vertebrae. This stepwise increase in vertebral number parallels a gradient of body shape from stout to slender and is ecologically mirrored by an extended aquatic phase, from ca. two months in *T. marmoratus* to ca. six months in *T. dobrogicus* (Arntzen, 2003; Wielstra et al., 2019). While these general trends are well-established, it is important to note that for some morphotypes supporting data remain sparse and that phenological variation among populations and years may be considerable (Jehle et al., 1997; Arntzen, 2024e; Naumov et al., 2025).

Cranial shape and feeding-related adaptations

Our results suggest a morphological continuum in skull shape across *Triturus* with no abrupt distinction between the *T. marmoratus* and *T. cristatus* species groups, despite a deep phylogenetic split of approximately 28 Mya. The observed continuum stretches from the marbled newt subspecies (*T. m. marmoratus*, *T. m. harmannis*), through pygmy newts (*T. pygmaeus*, *T. rudolfi*), to a series of crested newts (*T. karelinii* and allies, *T. carnifex* (*sensu lato*), *T. macedonicus*, *T. cristatus*, *T. dobrogicus*), in parallel to the above-described phenotypical series. Skull morphology ranges from short, broad crania with posteriorly positioned jaw articulations in the *T. marmoratus* species group to elongated skulls with more anterior jaw articulations in the highly aquatic

T. dobrogicus (Ivanović & Arntzen, 2014; this study).

The wide skulls with posterior jaw articulations characterise early salamanders (Schoch et al., 2020). Also, during ontogeny in many salamanders cranial skeleton undergo developmental transitions from larvae or juveniles with narrow and elongated skulls and anterior jaw articulations to broader skull of (semi-)terrestrial adults with laterally or posteriorly orientated jaw articulations (Reilly, 1996; Reilly & Lauder, 1990; Rose, 2003; Rose & Reiss, 1993; Djorović & Kalezić, 2000; Schoch et al., 2021). The same feature characterises early salamanders and Paleozoic tetrapods (Lebedkina, 1979; Schoch et al., 2020). In *Triturus* newts, the ontogenetic changes in skull shape between juveniles and adults are as described previously (Cvijanović et al., 2014), indicating that heterochronic changes could play a significant role in evolution of *Triturus* newts with the suction feeding in aquatic environment as a main driving force (Deban & Wake, 2000). For a similar scenario for the limb skeleton, see Ivanović et al. (2008).

Like many other salamanders, newts are traditionally recognised for capturing prey on land with their tongues or jaws and for using suction feeding in aquatic environments (Deban & Wake, 2000; Stinson & Deban, 2017; Wake & Deban, 2000). However, their complex life cycles including metamorphosis and adults that seasonally alternate between terrestrial hibernation and aquatic breeding phases (Duellman & Trueb, 1994) imply shifts in feeding strategies. During the terrestrial phase, salamanders enhance their adhesive system for efficient tongue-based prey capture, whereas in the aquatic breeding phase, this system regresses, precluding lingual prehension on land and shifting feeding to jaw-based pray capture (Heiss et al., 2013, 2017; Schwarz et al., 2023). The trade-off between these two environments can act as a constraint, reducing morphological specialization and diversification in skull shape among taxa that exhibit continuous variation in cranial morphology (Fig. 4).

The most divergent *Triturus* species, with an elongated skull and a more anteriorly positioned jaw articulation, is the highly aquatic *T. dobrogicus*. In aquatic salamanders, labial lobes help cover the lateral jaw areas (cheeks), enabling efficient, anteriorly directed suction feeding (Lauder, 1985; Van Wassenbergh & Heiss, 2016; Heiss et al., 2018). Species with more anteriorly placed jaw articulations require less lateral coverage to generate effective suction forces, which are primarily powered by hyobranchial depression. By contrast, species with larger, more posteriorly articulated jaws (such as those in the *T. marmoratus* group and the more terrestrial crested newt species), achieve a wider gape. Posteriorly positioned jaws may enhance the handling of large prey and facilitate more effective tongue projection. Comparative studies of feeding efficacy across different *Triturus* species and morphotypes, in both aquatic and terrestrial environments, could further clarify the ecological significance of these cranial adaptations.

In the *T. marmoratus* species group, skull shape variation is mainly restricted to internal features involved in feeding, such as the length and position of vomerine tooth rows, the placement of the pterygoid, and the relative position

of jaw articulation. These skeletal structures are closely associated with the feeding musculature: the jaw adductors (*m. adductor mandibulae externus* and *posterior*) attach to the squamosal, the *m. interhyoideus* to the quadrate, and the *m. levator bulbii* to the pterygoid (Francis, 1934; Iordansky, 1996, 2002). Variation in these elements likely reflects differences in feeding performance or dietary specialization (Cvijanović et al., 2014). Notably, the vomerine tooth rows length distinguishes the subspecies of *T. marmoratus* and also the sister species within *T. carnifex sensu lato* (see Fig. 4). It has been documented that *T. carnifex* (unlike some other species) uses its tongue to rasp prey against the vomerine dentition (Heiss et al., 2019; Schwarz et al., 2020a, 2023), underscoring the functional relevance of vomerine tooth row size and shape in food processing and ecological adaptation. In contrast to prey capture (suction in water vs. grasping on land), food processing in *T. carnifex* involving vomerine teeth has been shown to differ only slightly between the two environments (Schwarz et al., 2020b). Interestingly, the highly aquatic *T. dobrogicus* shows substantial intraspecific variation in vomerine tooth rows without phylogeographic structure, suggesting that a prolonged aquatic period may reduce the strength of selection acting on vomerine dentation. The prolonged aquatic period, apart from driving changes in skull shape for more efficient suction feeding, also imposes distinct demands on processing behaviour, leading to altered kinematics of food processing (Schwarz et al., 2020b). Furthermore, flexible responses to prey types that do not require extensive processing, may explain the observed variation in vomerine dentition in *T. dobrogicus*.

Marbled and pygmy newts: skull shape and ecological associations

Within the *T. marmoratus* species group, our study documents clear differences in skull shape among the five (sub)species, broadly aligning with recent taxonomic revisions (Arntzen, 2024abc). The most evident difference between marbled (*T. m. marmoratus*, *T. m. harmannis*) and pygmy newts (*T. p. pygmaeus*, *T. p. lusitanicus* and *T. rudolfi*) lies in body size (Arntzen, 2018; Ivanović et al., 2025), yet the documented skull shape differences are not allometric. Pronounced skull shape differences between subspecies pairs, such as *T. m. marmoratus* vs. *T. m. harmannis* and *T. p. pygmaeus* vs. *T. p. lusitanicus*, support this interpretation. Because these subspecies do not differ in skull size, their morphological divergence cannot be attributed to allometry and is more likely a consequence of ecological divergence. As noted above, the skeletal-muscular differences within the *T. marmoratus* species group are most likely related to feeding mechanics. Ecological differences between some taxa, such as those between *T. m. harmannis*, *T. p. lusitanicus* and *T. rudolfi*, have been documented in relation to hybrid zone structure and environmental limits to species ranges (Espregueira Themudo & Arntzen, 2007, 2012; Arntzen & Espregueira Themudo, 2008; Arntzen et al., 2021; López-Delgado et al., 2021) and it is plausible that local ecological pressures contribute to the observed cranial differences.

Morphological disparity on skull shape versus vertebral conservatism

One of the more unexpected findings of this study is the comparable level of skull shape disparity among the, in terms of axial morphology, uniform *T. marmoratus* species group relative to the diversity observed in the *T. cristatus* species group. This apparent decoupling between cranial and axial morphological evolution (Ivanović & Arntzen, 2014) suggests that along with body elongation and duration of the aquatic period, ecological/behavioural specialisation and possible trophic differentiation, may play key roles in driving skull shape evolution in *Triturus*, rendering this group of organisms a promising model system for investigating feeding mechanics.

Two main limitations that constrain our conclusions are a restricted geographic sampling as in *T. m. marmoratus*, and small sample sizes, notably for *T. rudolfi*. Future studies might target zones of contact and hybridisation, including those of *T. m. marmoratus* and *T. m. harmannis* and *T. carnifex* and its candidate sister species, as to offer insights into how functionally relevant traits evolve across ecological gradients and taxonomic boundaries.

Acknowledgements

We thank Rob Langelaan for assistance in the laboratory and an anonymous reviewer for constructive suggestions which enhanced the discussion on the functional aspects of feeding mechanics.

Supplementary Information

Representative 3D surface models for each (sub)species of *T. marmoratus* species group are available from MorphoSource (https://www.morphosource.org/projects/000780970?locale=en). Collection information followed by specimens ID is provided in parenthesis. Museum codes RMNH.RenA and ZMA.RenA – Naturalis Biodiversity Centre, Leiden, The Netherlands. *T. m. harmannis* (RMNH.RenA_51792), *T. m. marmoratus* (ZMA.RenA_9074_533), *T. rudolfi* (RMNH.RenA_51784), *T. p. lusitanicus* (ZMA.RenA_7615_178) and *T. p. pygmaeus* (ZMA.RenA_9087_40).

References

Adams, D., Collyer, M., Kaliontzopoulou, A. & Baken, E. (2025) Geomorph: software for geometric morphometric analyses. R package version 4.0.10. Available at https://cran.r-project.org/package=geomorph.

Arntzen, J.W. (2003) *Triturus cristatus* Superspezies – Kammolch Artenkreis (*Triturus cristatus* (Laurenti, 1768) – Nördlicher Kammolch, *Triturus carnifex* (Laurenti, 1768) – Italienischer Kammolch, *Triturus dobrogicus* (Kiritzescu, 1903) – Donau-Kammolch, *Triturus karelinii* (Strauch, 1870) – Südlicher Kammolch). In: K. Grossenbacher & B. Thiesmeier (Eds), *Handbuch der Reptilien und Amphibien Europas 4(2a): Schwanzlurche* (*Urodela*), pp. 421–514. Aula Verlag, Wiebelsheim, Germany.

Arntzen, J.W. (2018) Morphological and molecular characters to describe a marbled newt hybrid zone in the Iberian peninsula.

Contrib. Zool., 87, 167–185. https://doi.org/10.1163/18759866-08703003.

Arntzen, J.W. (2024a) Morphological and genetic diversification of Old-World marbled newts, with the description of a new and 'not-at-all-cryptic' subspecies from the Iberian Peninsula (*Triturus*, Salamandridae). *Contrib. Zool.,* 93, 127–152. https://doi.org/10.1163/18759866-bja10055.

Arntzen, J.W. (2024b) Morphological and genetic diversification of pygmy and marbled newts, with the description of a new species from the wider Lisbon Peninsula (*Triturus*, Salamandridae). *Contrib. Zool.,* 93, 178–200. https://doi.org/10.1163/18759866-bja10057.

Arntzen, J.W. (2024c) A subspecies of marbled newt (*Triturus marmoratus*) in the Iberian Peninsula newly resolved from congruent nuclear and mitochondrial DNA data. *Contrib. Zool.,* 93, 252–267. https://doi.org/10.1163/18759866-bja10060.

Arntzen, J.W. (2024d) Hybridization and introgression in deeply differentiated salamander species–molecular genetics and a reappraisal of Dr. Louis Vallée's osteological data. *Contrib. Zool.,* 93, 445–465. https://doi.org/10.1163/18759866-bja10067.

Arntzen, J.W. (2024e) On the aquatic phenology of sympatric crested and marbled newts (genus *Triturus*). *Amphibi. Reptil.*, 45, 501–506. https://doi.org/10.1163/15685381-bja10199.

Arntzen, J.W., Wielstra, B. & Wallis, G.P. (2014) The modality of nine *Triturus* newt hybrid zones assessed with nuclear, mitochondrial and morphological data. *Biol. J. Linn. Soc.,* 113, 604–622. https://doi.org/10.1111/bij.12358.

Arntzen, J.W., Beukema, W., Galis, F. & Ivanović, A. (2015) Vertebral number is highly evolvable in salamanders and newts (family Salamandridae) and variably associated with climatic parameters. *Contrib. Zool.,* 84, 85–113. https://doi.org/10.1163/18759866-08402001.

Arntzen, J.W. & Espregueira Themudo, G. (2008) Environmental parameters that determine species geographical range limits as a matter of time and space. *J. Biogeogr.*, 35, 1177–1186. https://doi.org/10.1111/j.1365-2699.2007.01875.x.

Arntzen, J.W., López-Delgado, J., van Riemsdijk, I. & Wielstra, B. (2021) A genomic footprint of a moving hybrid zone in marbled newts. *J. Zool. Syst. Evol. Res.*, 59, 459–465. https://doi.org/10.1111/jzs.12439.

Baken, E.K., Collyer, M.L., Kaliontzopoulou, A. & Adams, D.C. (2021) Geomorph v4.0 and gmShiny: enhanced analytics and a new graphical interface for a comprehensive morphometric experience. *Methods Ecol. Evol.,* 12, 2355–2363. https://doi.org/10.1111/2041-210X.13723.

Bardua, C., Wilkinson, M., Gower, D.J. Sherratt, E. & Goswami, A. (2019) Morphological evolution and modularity of the caecilian skull. *BMC Evol. Biol.,* 19, 30. https://doi.org/10.1186/s12862-018-1342-7.

Cheverud, J.M. (1995) Morphological integration in the saddle-back tamarin (*Saguinus fuscicollis*) cranium. *Am. Nat.,* 145, 63–89. https://doi.org/10.1086/285728.

Collyer, M.L. & Adams, D.C (2018) RRPP: an R package for fitting linear models to high-dimensional data using residual randomization. *Methods Ecol. Evol.,* 9, 1772–1779. https://doi.org/10.1111/2041-210X.13029.

Collyer, M.L. & Adams, D.C. (2024) RRPP: linear model evaluation with randomized residuals in a permutation procedure. R package version 2.1.2. Available at https://CRAN.R-project.org/package=RRPP.

Cvijanović, M., Ivanović, A., Kalezić, M. & L., Zelditch, M. (2014) The ontogenetic origins

of skull shape disparity in the *Triturus cristatus* group. *Evol. Dev.,* 16, 306–317. https://doi.org/10.1111/ede.12093.

Deban, S.M. & Wake, D.B. (2000) Aquatic Feeding in Salamanders. In: K. Schwenk (Ed.), *Feeding: Form, Function, and Evolution in Tetrapod Vertebrates*, pp. 65–94. Academic Press, San Diego, California, USA.

Djorović, A., & Kalezić, M.L. (2000) Paedogenesis in European newts (*Triturus*: Salamandridae): Cranial morphology during ontogeny. *J. Morphol.,* 243, 127–139. https://doi.org/10.1002/(SICI)1097-4687(200002)243:2<127::AID-JMOR2>3.0.CO;2–0.

Dryden, I.L. & Mardia, K.V. (1998) *Statistical Analysis of Shape*. John Wiley & Sons, Chichester, UK.

Duellman, W.E. & Trueb, L. (1994) *Biology of Amphibians*. Johns Hopkins University Press Baltimore, Maryland, USA.

Espregueira Themudo, G. & Arntzen J.W. (2007) Newts under siege: range expansion of *Triturus pygmaeus* isolates populations of its sister species. *Divers. Distrib.,* 13, 580–586. https://doi.org/10.1111/j.1472-4642.2007.00373.x.

Espregueira Themudo, G., Nieman, A.M. & Arntzen J.W. (2012) Is dispersal guided by the environment? A comparison of interspecific gene flow estimates among differentiated regions of a newt hybrid zone. *Mol. Ecol.,* 21, 5324–5335. https://doi.org/10.1111/mec.12026.

Fabre, A.C., Bardua, C., Bon, M., Clavel, J., Felice, R.N., Streicher, J.W., Bonnel, J., Stanley, E.L., Blackburn, D.C. & Goswami, A. (2020) Metamorphosis shapes cranial diversity and rate of evolution in salamanders. *Nature Ecol. Evol.,* 4, 1129–1140. https://doi.org/10.1038/s41559-020-1225-3.

Francis, E.B.T. (1934) *The Anatomy of the Salamander.* Clarendon Press, Oxford, UK.

Hallgrímsson, B., Jirik, F.R., Lieberman, D.E., Liu, W. & Ford-Hutchinson, A.F. (2007) Epigenetic interactions and the structure of phenotypic variation in the cranium. *Evol. Dev.,* 9, 91. https://doi.org/10.1111/j.1525-142X.2006.00139.x.

Heiss, E., Aerts, P. & Van Wassenbergh, S. (2013) Masters of change: seasonal plasticity in the prey-capture behavior of the Alpine newt *Ichthyosaura alpestris* (Salamandridae). *J. Exp. Biol.,* 216, 4426–4434. https://doi.org/10.1242/jeb.091991.

Heiss, E., Aerts, P. & Van Wassenbergh, S. (2018) Aquatic-terrestrial transitions of feeding systems in vertebrates: a mechanical perspective. *J. Exp. Biol.,* 221, jeb154427. https://doi.org/10.1242/jeb.154427.

Heiss, E., Schwarz, D. & Konow, N. (2019) Chewing or not? Intraoral food processing in a salamandrid newt. *J. of Exp. Biol.,* 222, jeb189886. https://doi.org/10.1242/jeb.189886.

Heiss, E., Handschuh, S., Aerts, P. & Van Wassenbergh, S. (2017) A tongue for all seasons: extreme phenotypic flexibility in salamandrid newts. *Sci. Rep.* 7, 1006. https://doi.org/10.1038/s41598-017-00674-y.

Iordansky, N.N. (1996) Evolution of the musculature of the jaw apparatus in the Amphibia. *Adv. Amph. Res. Former Soviet Union,* 1, 3–26.

Iordansky, N.N. (2002) Musculature of jaw apparatus in Urodela: variations in conservative system. *Zool. Zh.,* 81, 1494–1505 [In Russian].

Ivanović, A., Tomašević, N., Džukić, G., & Kalezić, M.L. (2008) Evolutionary diversification of the limb skeleton in crested newts (*Triturus cristatus* superspecies, Caudata, Salamandridae). *Ann. Zool. Fenn.*, 45, 527–535.

Ivanović, A. & Kalezić, M.L. (2012) Sexual dimorphism in skull geometry of newt species of *Ichthyosaura*, *Triturus* and *Lissotriton* (Salamandridae, Caudata, Amphibia). *Zoomorphology,* 131, 69–78. https://doi.org/10.1007/s00435-011-0143-y.

Ivanović, A., Üzüm, N., Wielstra, B., Olgun, K., Litvinchuk, S.N., Kalezić, M.L. & Arntzen, J.W. (2013) Is mitochondrial DNA divergence of Near Eastern crested newts (*Triturus karelinii* group) reflected by differentiation of skull shape? *Zool. Anz.,* 2252, 69–277. https://doi.org/10.1016/j.jcz.2012.08.005.

Ivanović, A., Vučić, T. & Arntzen, J.W. (2025) Allometry, sexual dimorphism, and Rensch's rule in pygmy and marbled newts. *J. Evol. Biol.,* 38, 240–250. https://doi.org/10.1093/jeb/voae150.

Ivanović, A. & Arntzen, J.W. (2014) The evolution of skull and body shape in *Triturus* newts reconstructed from 3D morphometric data and phylogeny. *Biol. J. Linn. Soc.,* 113, 243–255. https://doi.org/10.1111/bij.12314.

Ivanović, A. & Arntzen, J.W. (2018) Evolution of skull shape in the family Salamandridae (Amphibia: Caudata). *J. Anat.,* 232, 59–370. https://doi.org/10.1111/joa.12759.

Ivanović, A., Sotiropoulos, K., Vukov, T.D., Eleftherakos, K., Džukić, G., Polymeni, R.M. & Kalezić, M.L. (2008) Cranial shape variation and molecular phylogenetic structure of crested newts (*Triturus cristatus* superspecies: Caudata, Salamandridae) in the Balkans. *Biol. J. Linn. Soc.,* 95, 348–360. https://doi.org/10.1111/j.1095-8312.2008.01045.x.

Ivanović, A., Üzüm, N., Wielstra, B., Olgun, K., Litvinchuk, S.N., Kalezić, M.L. & Arntzen, J.W. (2013) Is mitochondrial DNA divergence of Near Eastern crested newts (*Triturus karelinii* group) reflected by differentiation of skull shape? *Zool. Anz.,* 2252, 69–277. https://doi.org/10.1016/j.jcz.2012.08.005.

Jehle, R., Pauli-Thonke, A., Tamnig, J. & Hödl, W. (1997) Phänologie und Wanderaktivität des Donaukammolches (*Triturus dobrogicus*). *Stapfia,* 51, 119–132.

Kazilas, C., Dufresnes, C., France, J., Kalaentzis, K., Martínez-Solano, I., de Visser, M.C., Arntzen, J.W. & Wielstra, B. (2024) Spatial genetic structure in European marbled newts revealed with target enrichment by sequence capture. *Mol. Phylogen. Evol.*, 194, 108043. https://doi.org/10.1016/j.ympev.2024.108043.

Klingenberg, C.P., Barluenga, M. & Meyer, A. (2002) Shape analysis of symmetric structures: quantifying variation among individuals and asymmetry. *Evolution,* 56, 1909–1920. https://doi.org/10.1554/0014-3820(2002)056[1909:SAOSSQ]2.0.CO;2.

Kyomen, S., Murillo-Rincón, A.P. & Kaucká, M. (2023) Evolutionary mechanisms modulating the mammalian skull development. *Phil. Trans. Roy. Soc. B,* 378, 20220080. https://doi.org/10.1098/rstb.2022.0080.

Landmark (2005) *IDAV Landmark Editor* 3.6 software. Institute for Data Analysis and Visualization, University of California, Davis, USA. https://www.cs.ucdavis.edu/~amenta/LandmarkDoc_v3_b6.pdf/.

Lauder, G. (1985) Functional morphology of the feeding mechanism in lower vertebrates. *Fortschr. Zool.*, 30, 179–188.

Lebedkina, N.S. (1979) *Evolution of the Amphibian Skull.* Nauka, Moscow, Russia. (In Russian).Translated and edited by Sergei V. Smirnov in 2004, Pensoft, Sofia, Bulgaria.

López-Delgado, J., van Riemsdijk, I. & Arntzen, J.W. (2021) Tracing species replacement in Iberian marbled newts. *Ecol. Evol.*, 11, 402–414. https://doi: 10.1002/ece3.7060.

Mayr, E. (1931) Remarks on the classification of the species of birds. *Proceedings of the 7th International Ornithological Congress*, 1, 246–247.

Mayr, E. (1942) *Systematics and the Origin of Species.* Columbia University Press, New York, USA.

Mertens, R. & Müller, L. (1928) Die Amphibien und Reptilien Europas. *Abh. Senckenb. Naturforsch. Ges.,* 41, 1–62.

Naumov, B.Y., Lukanov, S.P., Vacheva, E.D., Lazarkevich, I.V. & Slavchev, M.L. (2025) Phenology and sex ratio of *Triturus cristatus* (Laurenti, 1768) (Amphibia: Salamandridae) at its southern range limit. *Acta Zool. Bulg.,* 77, 71–84. https://doi.org/10.71424/azb77.1.002822.

Paluh, D.J., Stanley, E.L. & Blackburn, D.C. (2020) Evolution of hyperossification expands skull diversity in frogs. *Proc. Natl Acad. Sci. USA*, 117, 8554–8562. https://doi.org/10.1073/pnas.2000872117.

R Core Team (2024) *R: A Language and Environment for Statistical Computing*. R Foundation for Statistical Computing, Vienna, Austria. Available at https://www.R-project.org.

Reilly, S.M. (1996) The metamorphosis of feeding kinematics in *Salamandra salamandra* and the evolution of terrestrial feeding behavior. *J. Exp. Biol.,* 199, 1219–1227. https://doi.org/10.1242/jeb.199.5.1219.

Reilly, S.M. & Lauder, G.V. (1990) Metamorphosis of cranial design in tiger salamanders (*Ambystoma tigrinum*): a morphometric analysis of ontogenetic change. *J. Morph.* 204, 121–137. https://doi.org/10.1002/jmor.1052040202.

Rensch, B. (1929) *Das Prinzip geographischer Rassenkreise und das Problem der Artbildung*. Gebrüder Borntraeger, Berlin, Germany.

Rohlf, F.J. & Slice, D. (1990) Extensions of the Procrustes method for the optimal superimposition of landmarks. *Syst. Zool.,* 39, 40–59. https://doi.org/10.2307/2992207.

Rose, C.S. (2003) The developmental morphology of salamander skulls. In: H. Heatwole & M. Davies (Eds), *Amphibian Biology*, pp. 1684–1781. Surrey Beatty & Sons Pty Ltd. Sydney, Australia.

Rose, C.S. & Reiss, J.O. (1993) Metamorphosis and the vertebrate skull: ontogenetic patterns and developmental mechanisms. In: J. Hanken & B.K. Hall (Eds), *The Skull Development*, pp. 289–346. The University of Chicago Press, Chicago, USA.

Schoch, R.R., Pogoda, P. & Kupfer, A. (2021) The impact of metamorphosis on the cranial osteology of giant salamanders of the genus *Dicamptodon. Acta Zool.,* 102, 88–104. https://doi.org/10.1111/azo.12318.

Schoch, R.R., Werneburg, R & Voig, S. (2020) A Triassic stem-salamander from Kyrgyzstan and the origin of salamanders. *Proc. Natl Acad. Sci. USA.*, 117, 11584–11588. https://doi.org/10.1073/pnas.2001424117.

Sherratt, E., Gower, D.J., Klingenberg, C.P. & Wilkinson, M. (2014) Evolution of cranial shape in caecilians (Amphibia: Gymnophiona). *Evol. Biol.,* 41, 528–545. https://doi.org/10.1007/s11692-014-9287-2.

Sherratt, E. & Kraatz, B. (2023) Multilevel analysis of integration and disparity in the mammalian skull. *Evolution,* 77, 1006–1018. https://doi.org/10.1093/evolut/qpad020.

Stewart, A.A. & Wiens, J.J. (2025) A time-calibrated salamander phylogeny including 765 species and 503 genes. *Mol. Phyl. Evol.,* 204, 108272. https://doi.org/10.1016/j.ympev.2024.108272.

Stinson, C.M. & Deban, S.M. (2017) Functional morphology of terrestrial prey capture in salamandrid salamanders. *J. Exp. Biol.,*

220, 3896–3907. https://doi.org/10.1242/jeb.164285.

Schwarz, D., Konow, N., Porro, L.B. & Heiss, E. (2020a) Ontogenetic plasticity in cranial morphology is associated with a change in the food processing behavior in Alpine newts. *Front. Zool.*, 17, 34. https://doi.org/10.1186/s12983-020-00373-x.

Schwarz, D., Gorb, S.N., Kovalev, A., Konow, N. & Heiss, E. (2020b) Flexibility of intraoral food processing in the salamandrid newt *Triturus carnifex*: effects of environment and prey type. *J. Exp. Biol.,* 223: jeb232868. https://doi.org/10.1242/jeb.232868.

Schwarz, D., Heiss, E., Pierson, T.W., Konow, N. & Schoch, R.R. (2023) Using salamanders as model taxa to understand vertebrate feeding constraints during the late Devonian water-to-land transition. *Phil. Trans. Roy. Soc. B,* 378, 20220541. https://doi.org/10.1098/rstb.2022.0541.

Urošević, A., Ljubisavljević, K. & Ivanović, A. (2019) Multilevel assessment of the Lacertid lizard cranial modularity. *J. Zool. Syst. Evol. Res.,* 57, 145–158. https://doi.org/10.1111/jzs.12245.

Üzüm, N., Ivanović, A., Gümüş, Ç., Avci, A. & Olgun, K. (2015) Divergence in size, but not in shape: variation in skull size and shape within *Ommatotriton* newts. *Acta Zool.,* 96, 478–486. https://doi.org/10.1111/azo.12092.

Van Wassenbergh, S. & Heiss, E. (2016) Phenotypic flexibility of gape anatomy fine-tunes the aquatic prey-capture system of newts. *Sci. Rep.* 6, 29277. https://doi.org/10.1038/srep29277.

Wallis, G.P. & Arntzen, J.W. (1989) Mitochondrial-DNA variation in the crested newt superspecies: limited cytoplasmic gene flow among species. *Evolution,* 43, 88–104. https://doi.org/10.1111/j.1558-5646.1989.tb04209.x.

Wake, D.B. & Deban, S.M. (2000) Terrestrial feeding in salamanders. In: K. Schwenk (Ed.), *Feeding: Form, function and evolution in tetrapod vertebrates*, pp. 95–116. Academic Press, San Diego, California, USA.

Wickham, H. (2016) *Ggplot2: Elegant Graphics for Data Analysis*. Springer-Verlag, New York, USA. https://doi.org/10.1007/978-3-319-24277-4_9.

Wickham, H., François, R., Henry, L., Müller, K. & Vaughan, D. (2023) Dplyr: A grammar of data manipulation. R package version 1.1.4. Available at https://CRAN.R-project.org/package=dplyr.

Wielstra, B., Litvinchuk, S. N., Naumov, B., Tzankov, N., & Arntzen, J.W. (2013) A revised taxonomy of crested newts in the *Triturus karelinii* group (Amphibia: Caudata: Salamandridae), with the description of a new species. *Zootaxa, 3682,* 441–453. https://doi.org/10.11646/zootaxa.3682.3.5.

Wielstra, B., McCartney–Melstad, E., Arntzen, J.W., Butlin, R.K. & Shaffer, H.B. (2019) Phylogenomics of the adaptive radiation of *Triturus* newts supports gradual ecological niche expansion towards an incrementally aquatic lifestyle. *Mol. Phyl. Evol.,* 133, 120–127. https://doi.org/10.1016/j.ympev.2018.12.032.

Wielstra, B., Salvi, D. & Canestrelli, D. (2021) Genetic divergence across glacial refugia despite interglacial gene flow in a crested newt. *Evol. Biol.,* 48, 17–26. https://doi.org/10.1007/s11692-020-09519-5.

Wolterstorff, W. (1923) Übersicht den Unterarten und Formen des *Triton cristatus* Laur. *Blätter für Aquarien- und Terrarienkunde* 34, 120–126.

Appendix 1

Collection material of crested and marbled newts (sub)species that was re-analyzed in this study, ordered by species name, collection and locality information, followed by specimens ID [in square brackets]. Museum codes are: IBISS – Institute for Biological Research "Siniša Stanković" collection, Belgrade, Serbia; RMNH.RenA and ZMA.RenA – Naturalis Biodiversity Centre, Leiden, The Netherlands. *N* = sample size.

Triturus anatolicus: N =25, IBISS: Serefiye, Turkey [22444–22449, 22452], Kastamonu, Turkey [22847–48, 22852, 22854–55], Kalecik, Turkey [k22479, k22482–83, k22485–86]; Reşadiye, Turkey [r22511, r22513, r22517, r22519], ZMA.RenA: Reşadiye, Turkey [9186_k1, k2], Serefiye, Turkey [9187_a, b].

Triturus carnifex: N = 16, IBISS: Podstrmec, Slovenia [c11 (1, 11, 12, 15, 19)], Velika Vala, Croatia [c35 (2, 3, 5, 6, 8, 9, 11–15)].

Triturus 'carnifex', the Apennine sister species of *T. carnifex*, yet to be described: *N* = 14, ZMA.RenA: Popoli, Aquila, Italy [7553_71-76, 9107_780], Florence, Italy [9107_782-83], Fuscaldo, Italy [9108_405-09].

Triturus cristatus: N = 36, IBISS: Kamenskoye village, Ukraine [cr1, 232, 234, 251, 267, 304, 306], Miroč, Serbia [20051–51, 20065–66, 20074, 20076], ZMA.RenA: Slaskie, Mogelica, Poland [6276, 6282, 6284, 6286, 6288], Gaddesby, Leicestershire, UK [9285_1-10, 9285_12, 9285_14], Wijnandsrade, Limburg, The Netherlands [9313_a-d].

Triturus dobrogicus: N = 27, IBISS: Ivanovo, Serbia [c10 (4, 7, 14, 18, 23)], Insula, Romania, [ins (3, 5, 6, 8, 9)], ZMA.RenA: Belgrade, Serbia [9090_298-99; 9090_310, 9090_312], Öcsöd, Hungary [9141_365, 9141_967], Senta, Serbia [9153_427-34, 9153_437, 9153_511, 9153_745].

Triturus ivanbureschi: N = 27, IBISS: Claros, Turkey [22530–31, 22533, 22535–38], Bursa, Turkey [22866–67, 22870–73], Afyon, Turkey [22885–22887], RMNH.RenA: Ostar Kamak, Bulgaria [47200-03, 47210, 47212].

Triturus karelinii: N = 18, IBISS: Ersi, Tabasarinskii, Dagastan [22814-21], Kutuzovskoe Lake, Krym, Ukraine [22833, 22834-36], Locality unknown, Georgia [22242-44], Akhaldaba, Georgia [9343a,b], ZMA.RenA: Dizabad village [2389].

Triturus macedonicus: N = 26, IBISS: Rid, Montenegro [c30 (2, 5, 12, 15, 16)], Zagori, Greece [Zg (3, 4, 6, 10, 11)], ZMA.RenA: Ano Kaleniki, Greece [9085_661, 9085_658], Višegrad, Bosnia and Hercegovina [9118_896, 9118_898-99, 9118_900-09, 9118_962], Lučane, Montenegro [9137_809].

Triturus marmoratus marmoratus: N = 26, ZMA.RenA: Marcillé-la-Ville, Mayenne, France [7418_9–7418_14], Mayenne city, France [8002_a,b,c, 9074_325, 325, 466, 467, 468, 469, 533, 534, 539, 939], Jublains, Mayenne, France [9266_264, 265, 270, 271], Les Chênes Secs, Laval, Mayenne, France [9267_266, 267, 268].

Triturus marmoratus harmannis: N = 14, RMNH.RenA: Arrochela, Portugal [51792–51798], ZMA.RenA: El Burrueco, Spain [7614_161–7614_167, 71614_nl].

Triturus pygmaeus pygmaeus: N = 18, ZMA.RenA: Puerto de Galiz, Spain [7676_1–7676_10], halfway Archidona and Loja, Spain [9087_40–9087_44, 9087_46–9087_49, 9087_51].

Triturus pygmaeus lusitanicus: N = 22, RMNH.RenA: Olhos de Água, Portugal [22576–22579], ZMA.RenA: Villalba, Spain [7615_168, 7615_170, 7615_171, 7615_173–7615_178], Venta del Charco, Spain [7677_11–18, 7677_20].

Triturus rudolfi: N = 10, RMNH.RenA: Cercal, Portugal [51784–51791, 51793].